A Nanochannel Array-Based Electrochemical Device for Quantitative Label-free DNA Analysis

Su-Juan Li,[†] Jing Li,[†] Kang Wang,[*,†] Chen Wang,[†] Jing-Juan Xu,[†] Hong-Yuan Chen,[†] Xing-Hua Xia,[*,†] and Qun Huo[‡]

[†]Key Laboratory of Analytical Chemistry for Life Science, School of Chemistry and Chemical Engineering, Nanjing University, Nanjing 210093, China, and [‡]Nanoscience Technology Center, Department of Chemistry, Department of Materials, Mechanical and Aerospace Engineering, University of Central Florida, 12424 Research Parkway Suite 422, Orlando, Florida, United States

ABSTRACT A strategy for label-free oligonucleotide (DNA) analysis has been proposed by measuring the DNA-morpholino hybridization hindered diffusion flux of probe ions $Fe(CN)_6^{3-}$ through nanochannels of a porous anodic alumina (PAA) membrane. The flux of $Fe(CN)_6^{3-}$ passing through the PAA nanochannels is recorded using an Au film electrochemical detector sputtered at the end of the nanochannels. Hybridization of the end-tethered morpholino in the nanochannel with DNA forms a negatively charged DNA—morpholino complex, which hinders the diffusion of $Fe(CN)_6^{3-}$ through the nanochannels and results in a decreased flux. This flux is strongly dependent on ionic strength, nanochannel aperture, and target DNA concentration, which indicates a synergetic effect of steric and electrostatic repulsion effects in the confined nanochannels. Further comparison of the probe flux with different charge passing through the nanochannels confirms that the electrostatic effect between the probe ions and DNA dominates the hindered diffusion process. Under optimal conditions, the present nanochannel array-based DNA biosensor gives a detection limit of 0.1 nM.

KEYWORDS: nanochannel array · porous anodic alumina membrane · label-free sensor · morpholino · DNA · electrochemical analysis

The introduction of biomolecules into solid-state nanopores and nanochannels provides an interesting platform for studying the biosensing process and developing bioelectronic devices in confined nanospace. Biomolecule functionalized single nanopores have been successfully applied in the development of molecular or ionic gate,[1,2] biosensing[3,4] devices, and single molecule analysis prototypes.[5] Developing nanochannel array-based bioanalytical devices is an alternative approach to achieve high sensitive detection of biomolecules. A representative material of a nanochannel array is porous anodic alumina (PAA), whose channel density, radius, and length−radius ratio could be easily controlled during the fabrication process.[6] Au nanotubes formed along the nanochannels in the PAA membrane have been used to modulate molecular transport, recognition, and separation.[7,8] For the bare PAA membrane, direct modification of the nanochannels with chemical and biochemical molecules using silane chemistry is also developed. Label-free DNA detection[9] and electro-osmotic flow manipulation[10] have been reported using the direct modified PAA nanochannels. These applications mainly depend on the regulation of ion transport through nanochannels.[11−14] Therefore, understanding of the physical and chemical interaction between ions and the nanochannels is fundamentally important for developing new analytical methods and devices based on materials with confined nanospace.

Generally, the ion or molecule flux passing through a biofunctionalized nanopore or nanochannel is affected by the steric effect[15] and/or the electrostatic effect.[9,16,17] The former occurs when the modified biomolecule is comparable with the pore diameter, which results in a reduced effective ion-transporting region. The electrostatic effect is relatively a long-range effect caused by the attracting or repulsing interaction between the surface-immobilized charged molecules and the transporting ions; therefore, its occurrence depends less on the pore or channel size and can be modulated by altering the surface charge of the nanospace or ionic strength of the bulk solution. Both of these effects lead to a change of the ion mobility in the confined nanospace. So far, they have been widely used in nanopores for biomolecule sensing of organic polymers, proteins, peptides, and bioaffinity molecules.[18] If the electrostatic effect introduced by the biorecognition reaction is manipulated to block the ion flux as the steric effect does, the detection sensitivity of the nanochannel-based devices can be further improved.

*Address correspondence to wangkang@nju.edu.cn, xhxia@nju.edu.cn.

Received for review May 13, 2010 and accepted October 11, 2010.

Published online October 19, 2010. 10.1021/nn101050r

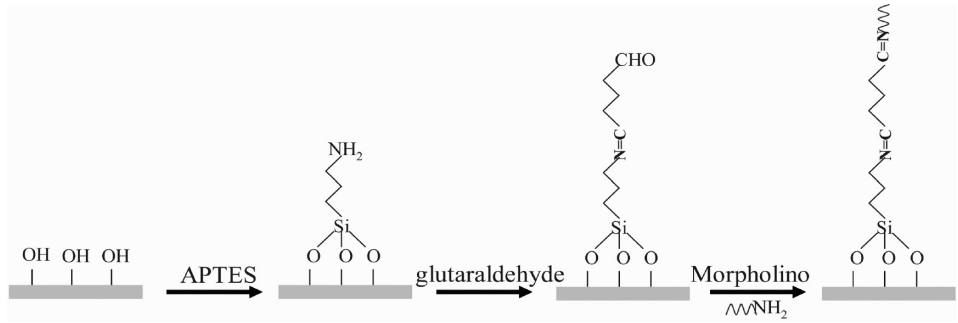

Scheme 1. Functionalization of the inner walls of PAA nanochannels with aminated morpholino.

A variety of detection methods have been developed to detect ion mobility in nanochannels. A relatively traditional detection approach is to measure the ionic current flowing through nanochannels. However, the existence of high ion/electrode interface resistance limits the further improvement of detection sensitivity.[19] Jagerszki *et al.* reported an optical method for flux detection in which the DNA hybridization modulated diffusion flux of fluorescent marker ions passing through Au nanotubes.[20] Subsequently, Smirnov *et al.* demonstrated a facile method for DNA detection by measuring ionic conductance directly through the nanochannels with both sides of a PAA membrane sputtered with gold as detection electrodes. Such a strategy effectively minimized the influence of solution resistance outside the pore on the ionic conductance measurement.[9]

Here, we present an *in situ* electrochemical detection system for measuring the flux of electroactive probe ions flowing through a morpholino (a neutral analogue of DNA)-anchored PAA nanochannel array for quantitative DNA sensing based on steric and electrostatic effects. Scheme 1 shows the procedure for functionalization of a PAA nanochannel with morpholino. The PAA membrane is employed due to its high pore density and well-organized tunable nanoarray channels. In addition, the mechanical stability of the PAA membrane enables a thin layer of Au film sputtered on one side of it which acts as an electrochemical detector. As generally known, the commercially available PAA membranes have a thickness of about 60 μm with 200-nm pores in one side (~59 μm in depth) and 20-nm pores in the other side (~1 μm depth).[21] As shown in Figure 1A,B, when the Au film electrode was sputtered on the 20 nm side, most of the channel opening was blocked. To avoid this unwanted blocking effect caused by the sputtered Au film, the 200 nm side of the commercial PAA membrane is used for the Au film sputtering. In this case, the sputtered Au film can hardly affect the size of the channel opening as indicated in Figure 1C,D. A comparison of Figure 1C with Figure 1D shows that the Au film sputtered on the 200 nm side exhibits good uniformity and the morphology of the Au film is dependent on the surface state of the substrate membrane. Such an Au film electrode shows very well the stability in our experiments even after being routinely used for 2 weeks. This detection design enables real time monitoring of the electroactive ion flux.

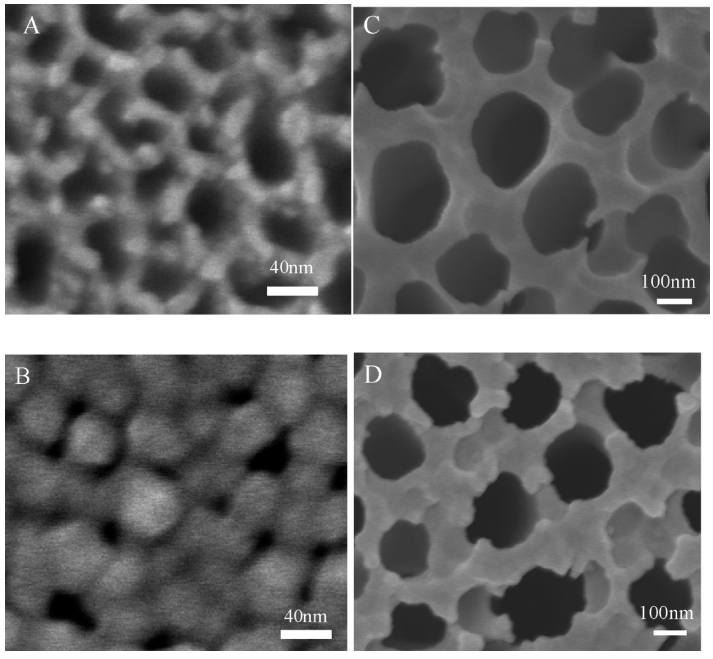

Figure 1. SEM images of both sides of the commercial PAA membrane before (A and C) and after (B and D) sputtering 100 nm thickness of gold film: (A, B) 20 nm side; (C, D) 200 nm side.

A low ionic strength is desired for achieving high detection sensitivity in the present device. Therefore, a neutral bioprobe morpholino is attached inside the nanochannel to capture target DNA, and negatively charged $Fe(CN)_6^{3-}$ is used as the electroactive probe to give an electrochemical signal. Because of its neutral nature, morpholino can form a stable double-strand structure with its cDNA even in very low ionic strengths,[22] which enables the change of the electrostatic effect being studied in low ionic strengths. $Fe(CN)_6^{3-}$ solution is filled in the feeding cell to create a concentration gradient which drives $Fe(CN)_6^{3-}$ transporting through the nanochannels to the Au film detector. A reduction potential of 0 V is used to detect the $Fe(CN)_6^{3-}$ (Supporting Information, Figure S2), where the electrochemical reaction of $Fe(CN)_6^{3-}$ is diffusion controlled, and the current response is directly propor-

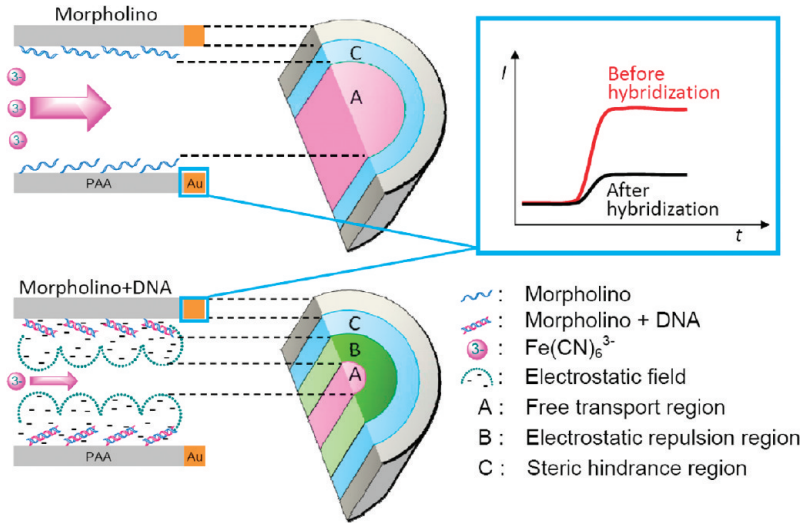

Scheme 2. Schematic representation of the working principle for the label-free DNA detection system using an electrochemical detector.

tional to the concentration of $Fe(CN)_6^{3-}$. Thus, the steady-state reduction current reflects the diffusion flux (J) of $Fe(CN)_6^{3-}$ across the nanochannels. J has the form of

$$J = mD\left(\frac{\partial[c_{Fe(CN)_6^{3-}}]}{\partial x}\right) \quad (1)$$

$$I = nFAJ = nFmAD\left(\frac{\partial[c_{Fe(CN)_6^{3-}}]}{\partial x}\right) \quad (2)$$

where A is the area in the nanochannel where the $Fe(CN)_6^{3-}$ can diffuse without hindrance; m is the number of nanochannels of the PAA membrane exposed in solution; D is the diffusion coefficient of $Fe(CN)_6^{3-}$; F is the Faradaic constant; n and c are the electron transfer number and concentration of $Fe(CN)_6^{3-}$, respectively; and x is the distance. D, m, and $\partial c/\partial x$ remain the same for a given concentration of $Fe(CN)_6^{3-}$ and PAA membrane. Therefore, the steady-state current, I, is proportional to the free transport area A.

RESULTS AND DISCUSSION

As depicted in Scheme 2, a layer of morpholino covers the inner wall of the PAA nanochannel before hybridization. The cross section of the PAA nanochannel thus can be divided into two regions: the steric hindrance region (C) and free transport region (A). Here, the area of free transport region, A, can be expressed as

$$A = \pi(r_{np} - r_{st})^2 \quad (3)$$

where, r_{np} is the pore radius of the nanochannel and r_{st} is the length of steric inhibition caused by the presence of the morpholino layer (the steric inhibition effect of the morpholino layer is confirmed negligible in a later section) or the morpholino−DNA layer (after hybridization).

Upon hybridization, the negatively charged DNA−morpholino double-strand layer in the nanochannel attracts cations and repels anions, forming a negatively charged electric field (region B in Scheme 2) in which the $Fe(CN)_6^{3-}$ anions have less chance to be found than that in the free transport region A. We name this region B as the electrostatic repulsion region. Such a newly generated hindrance region will decrease the pathway of anion passing through the nanochannels and result in a decreased flux of $Fe(CN)_6^{3-}$. The thickness of the region B (r_{rep}) greatly depends on the Debye shielding length, r_D, which has the form[23]

$$r_D = \sqrt{\frac{\varepsilon RT}{2\rho F^2 I b}} \quad (4)$$

where I is the ionic strength of the electrolyte, ε is the dielectric constant of the solution, and b is the mass molarity. Other parameters have their normal definitions. r_D is well-known to be modulated by changing the ionic strength. Therefore, the value of r_{rep} is also affected by the ionic strength. It is worth mentioning that the r_{rep} should not be considered equal to r_D because the Debye shielding length is obtained from the point of view of charge distribution in a static state, r_{rep} is a parameter depicting the region in which the same charged ions cannot freely diffuse through. The Debye−Hückel model considers that, in the ionic atmosphere, the electrostatic interactions only impose some degree of order over the randomly thermal motions but not completely block the ion movement.[24] That is, r_{rep} should be smaller than r_D. To simplify the expression, we connect r_{rep} and r_D using a coefficient γ, which is defined as

$$\gamma = r_{rep}/r_D \quad (5)$$

Therefore, the area of the free transport region A after hybridization can be expressed as

$$A = \pi(r_{np} - r_{st} - \gamma r_D)^2 \quad (6)$$

Consequently, under optimal conditions, the flux of

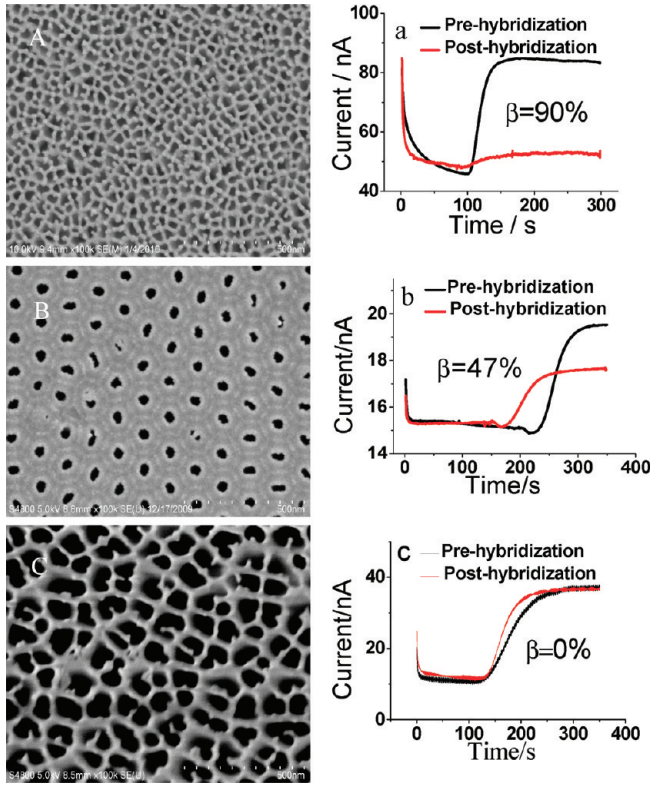

Figure 2. The effect of pore size on DNA quantitative analysis is shown in these SEM images. Panels a, b, and c were the steady-state reduction currents of $Fe(CN)_6^{3-}$ flowing through the morpholino-functionalized membrane of (A) 20 nm Whatman PAA membrane, (B) 40 nm self-made PAA membrane, and (C) 100 nm Whatman PAA membrane before and after incubation in 100 nM complementary ssDNA solution for 1 h. Final concentration of 0.03 mM $K_3Fe(CN)_6$ was added in the feeding cell filled with 0.5 mM Tris-HCl (pH8.0) against a plain buffer solution in the receiving cell. 0 V was used as the detection potential.

$Fe(CN)_6^{3-}$ passing through nanochannels decreases significantly, resulting in a smaller steady-state current response.

To achieve optimal performance of the present biosensing device, various factors influencing the ion flux passing through the nanochannel array were investigated. β, the decrease ratio of steady-state current due to DNA hybridization is defined by $\beta = 1 - I/I_0$, where I_0 and I are the current increases measured before and after hybridization. Because the current response of $Fe(CN)_6^{3-}$ is directly proportional to the free transport area in nanochannels, the pore size will considerably affect the β value. The results are shown in Figure 2. For a 20 nm PAA nanochannel array, the DNA−morpholino hybridization causes a 90% decrease in β value. In this case, most of the $Fe(CN)_6^{3-}$ ions are repelled from the nanochannels, indicating that the diffusion hindrance areas inside the nanochannels account for most of the nanochannels area. For the nanochannel array with the pore size of 40 nm, a β value of 47% is obtained. It can be estimated that nearly half of the area inside the nanochannel is effective for $Fe(CN)_6^{3-}$ free transport. However, with the pore size further increasing to 100 nm, no current change is observed. This observation shows that the diffusion hindrance regions are negligible as compared to the 100 nm diameter of pore size. Therefore, PAA membranes with a pore diameter of 20 nm were used for DNA quantitative analysis in the subsequent experiments.

As described in eqs 4 and 6, the ionic strength would directly influence the Debye shielding length and the area of the electrostatic repulsion region. For DNA analysis using the present scheme, a strong inhibition of probe ion transport caused by DNA binding is preferred for enhancing detection sensitivity. Thus, the influence of ionic strength on steady-state current of ferricyanide was investigated. The results are shown in Figure 3A. Before hybridization, I_0 is independent of ionic strength, probably due to the nearly uncharged morpholino-functionalized nanochannels. The isoelectric point of PAA is about pH 8.0.[25] In our experiment, it is found that the flux of $Fe(CN)_6^{3-}$ transporting through a bare PAA membrane still increases with the increase of ionic strength in pH 8.0 solution (Supporting Information, Figure S4). Hence, the inner wall of the nanochannel array that we used is a little negatively charged under our experimental conditions. With further modification of the membrane with amino silane and gluteraldehyde, the surface charge still exists and shows only a tiny change.[9] Then, a neutral molecule, morpholino, anchoring to the nanochannels will not contribute any charge. In addition, the morpholino monolayer covering the wall of the nanochannel will screen the small quantity of the original negative charge of PAA membrane, making the morpholino monolayer modified nanochannels a nearly neutral surface.

Interestingly, an obvious influence of ionic strength on the steady-state current of ferricyanide ion transporting through the DNA−morpholino hybridized nanochannels is observed (Figure 3A, filled cycles). The negatively charged morpholino−DNA surface induces formation of electrical field which makes the probe ion flux through the nanochannels very sensitive to ionic strength. As shown in Figure 3A, the current I shows a considerable decrease compared with I_0 at low ionic strength and then gradually recovers at relatively high ionic strength. However, a nearly 9% current decrease can still be observed compared with I_0 even in 80 mM ionic strength solutions (Figure 3B). This decrease of the steady-state current in high ionic strength can hardly be attributed to the electrostatic repulsion but more possibly comes from the steric inhibition due to the increase of diameter and rigidity from single-strand morpholino to double-strand DNA−morpholino inside the nanochannels. The further significant decrease in current response in lower ionic strength solutions for the DNA−morpholino system can thus be attributed to the electrostatic repulsion effect between DNA and $Fe(CN)_6^{3-}$. On the basis of the above analysis, it can be confirmed that the observed inhibition effect in Figure

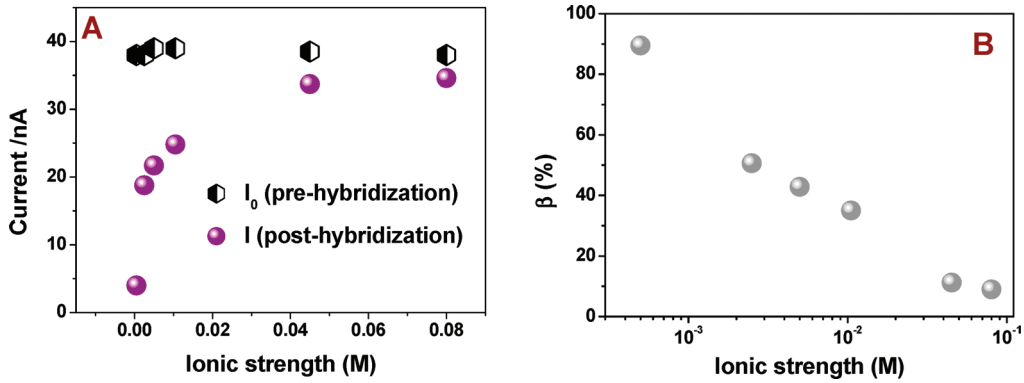

Figure 3. (A) The influence of ionic strength on current response of $Fe(CN)_6^{3-}$ transporting through morpholino-functionalized PAA membrane (20 nm) before and after hybridization with 100 nM ssDNA. The adjustment of ionic strength was performed by varying concentrations of NaCl. Other conditions were the same as in Figure 2. (B) The relationship of β with ionic strength; data are obtained from Figure 3A.

2 can be mainly ascribed to the electrostatic effect, especially in a large diameter of nanochannels. In other words, the electostatic repulsion force dominates the inhibition effect in low ionic strengths.

Because the steric effect of morpholino−DNA is observed in high ionic strength solution, the steric inhibition effect caused by the immobilization of single-strand morpholino in a nanochannel was also studied. In a high ionic strength solution, the modification of morpholino in the 20 nm nanochannels does not show a distinguishable effect on the $Fe(CN)_6^{3-}$ transport (Supporting Information, Figure S5). Because of the similar backbone structure of DNA and morpholino, it is reasonable to assume that morpholino molecules have a similar contour length with the DNA molecules which bear the same number of bases. Therefore, the 25mer morpholino used in the present research is about 6.25−11.00 nm long.[26] If the morpholino inside the nanochannels takes a stretched conformation, an obvious decrease of the steady-state current caused by the steric effect should be seen after the morpholino attachment. This phenomenon suggests that the morpholino inside the nanochannels have a conformation not extending to the solution but laying on the inner wall of the nanochannels. Such deduction is supported by researches reporting that ssDNA bases can adsorb on materials such as gold, carbon nanotube, and graphene.[27−30] Bearing such a conformation inside PAA nanochannels, it is not surprising that the steric inhibition effect of morpholino cannot be observed in 20 nm morpholino-modified nanochannels. This result confirms our initial hypothesis that interactions between the morpholino-modified nanochannels and transporting $Fe(CN)_6^{3-}$ is negligible. To observe the steric effect dominated inhibition effect, much smaller pore size is required and a single nanochannel may give more detailed information on molecule conformation inside the confined space.

For further quantitative illustration of the steric and electrostatic repulsion effects, different charged electroactive probes were investigated for DNA hybridization analysis (Figure 4). It can be found that the β value of neutral charged hydroquinone (HQ) and negatively charged ferricyanide ion are about 4% and 33.3%, respectively. These results further confirm that the electrostatic repulsion effect is dominant over the hindrance process for the negatively charged probe. On the contrary, for positively charged probe $Ru(NH_3)_6^{3+}$, $\beta = -7\%$ is obtained, indicating the probe flux increases after hybridization. This can be ascribed to the fact that the negatively charged DNA−morpholino nanochannel selectively allows the positively charged ions to permeate preferentially for maintaining the electroneutral condition in the nanochannel.[31] This demonstrates that the selection of $K_3Fe(CN)_6$ as an electroactive probe can increase the detection sensitivity.

Under optimal conditions of 0.5 mM buffer, the feasibility of the present nanochannel array-based sensor for quantitative DNA analysis was evaluated. Different concentrations of complementary single-strand DNA were used to hybridize with the morpholino-modified nanochannel array. The chronoamperometric technique always gives a decreasing current because the charging current occurring at the electrode/solvent interface decreases exponentially with time, but with time extension, a relatively steady-state current can be obtained. As shown in Figure 5, the steady-state current of $Fe(CN)_6^{3-}$ gradually decreases with the concentration of the cDNA increasing from 0.1 nM to 100 nM. Such a response indicates that more DNA−morpholino double strands are formed inside the nanochannels with the increase of the DNA concentration. The increase of the surface charge density, though not changing the Debye length, increases the possibility of $Fe(CN)_6^{3-}$ ions being repelled by the negatively charged DNA−morpholino double strands inside the nanochannels.[32] Accordingly, a low steady-state current is obtained. A 90% current decrease is achieved upon hybridizing in 100 nM of cDNA solution; however, no signal change is observed after hybridizing in non-cDNA solution. These results show that the present morpholino-functionalized nanochannel arrays are

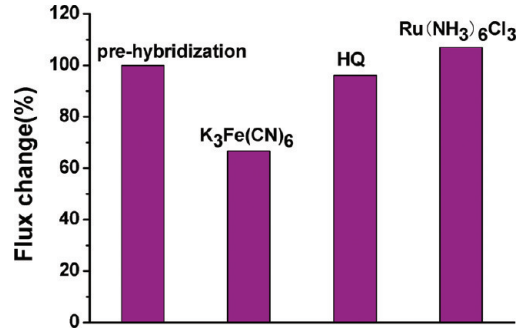

Figure 4. The current change of different charged probes through a morpholino-functionalized PAA membrane after hybridizing with 10 nM cDNA for 1 h. A final concentration of 0.03 mM of the probe was added in the feeding cell filled with 0.5 mM Tris-HCl (pH8.0) against a plain buffer solution in the receiving cell.

highly selective as a DNA biosensor. Therefore, it is possible that the flux of $Fe(CN)_6^{3-}$ will be completely blocked (switch off state) if higher DNA surface density can be obtained or a smaller nanochannel is used. After the membrane is treated with 9 M urea, the current signal recovers to the initial value (switch on state, Figure 5B). In this case, the DNA sensor behaves like a nanovalve for specific ions,[2] and the extent of switch can be modulated by the concentrations of incubated cDNA. However, because of the strong binding force of morpholino−DNA, it is always difficult to fully make the membrane dehybridization. Therefore, with repeating denaturing processes, the membrane is hardly renewed to its initial properties. But if a longer time for dehybridization process is used, a relatively similar behavior of ion transport as that without hybridization can be achieved.

For nanochannel array-based biosensors that bear low pore density, the anchored bioprobes on the outer surface of membrane are also a limitation factor for detection of low concentrations of target analyst. Because analytes that react with the bioprobes which are attached on the outer surface of the membrane do not contribute to signal change.[20] However, for well-fabricated anodic aluminum oxide membranes, it possesses a much higher pore density up to ~10^{11} pores/cm^2 and a narrower distribution of channel diameters.[10] For a 20 nm PAA membrane, it can be estimated that the internal surface area is about 10^4 times larger than the area of its outer surface. Therefore, the amount of bioprobes immobilized on the outer surface is negligible compared with the ones incubated inside the nanochannels. Thus, in our experiment, even with low concentrations of cDNA (0.1 nM), significant change in steady-state current can be observed in the 20 nm nanochannel array.

Fast response speed and low detection limit are desired features for a good sensor. In most of the nanochannel array-based researches, the probe molecules were detected in the receiving cell instead of directly detected inside the nanochannels. In such a case, the probe concentration is greatly diluted by the buffer solution before being detected.[33,20] Therefore, these methods have a higher detection limit and longer response time[34] (10 min in ref 20, for example). Compared with these detection methods, our real time electrochemical detection method is more convenient, sensitive, and bears a fast response speed (about 50 s) thanks to the good positioning of the detector which was directly integrated at the end of the nanochannels. As soon as $Fe(CN)_6^{3-}$ ions diffuse across the nanochannel, they can be immediately detected on the Au film electrode. The reliable detection limit of this DNA sensor is 10^{-10} M (as shown in Figure 6), which is comparable to the optical method with PNA as the recognition site in 14 nm Au nanotubes. We believe such a low detection limit also profits from the high valence $Fe(CN)_6^{3-}$ probe, which leads to strong electrostatic interactions with DNA-functionalized nanochannels based on Donnan exclusion model.[25,35] On the other hand, the nearly zero charged surface of morpholino-functionalized nanochannels provides a blank background, which also improves the detection sensitivity for sensing DNA−morpholino hybridization. In principle, a further decreasing of the nanochannel diameter of PAA mem-

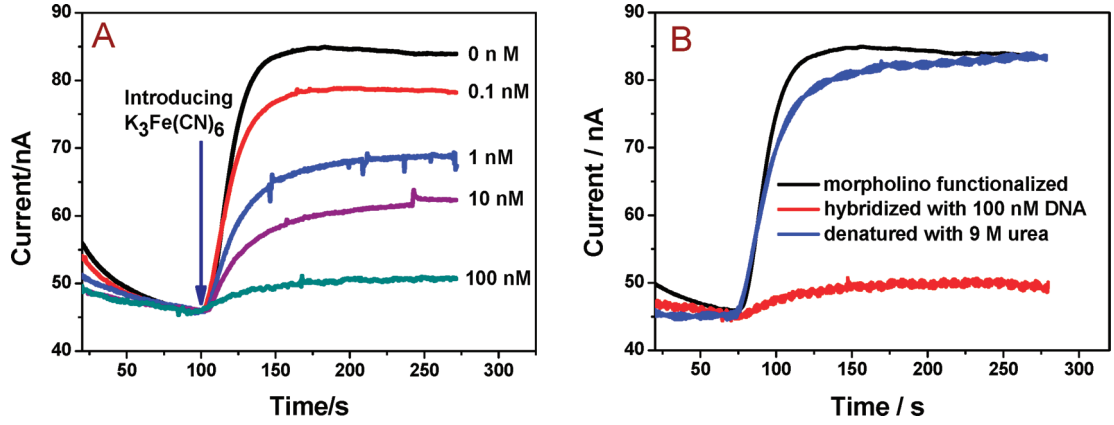

Figure 5. The steady-state current response of the morpholino-functionalized nanochannel array after hybridizing in different concentrations of cDNA (A) and before and after denaturation of double strand in 9 M urea (B). A 20 nm PAA nanochannel array was used. Other conditions were the same as in Figure 2.

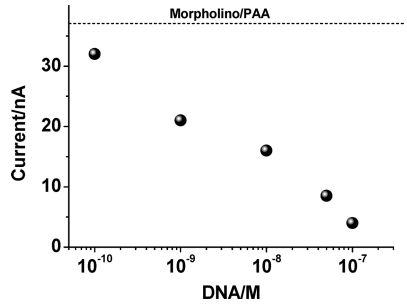

Figure 6. Dependence of current response for $Fe(CN)_6^{3-}$ on the cDNA concentration. Other conditions are the same as in Figure 5.

branes can also improve the detection sensitivity and detection limit.

CONCLUSIONS

We demonstrate a real time electrochemical system for detecting the interactions between DNA−morpholino-modified nanochannels and ferricyanide probe ions. Our results show that these interactions can effectively modulate the transport properties of negatively charged $Fe(CN)_6^{3-}$ ions flowing through the nanochannels. Based on these observations, a label-free DNA sensor has been successfully constructed. The steady-state current caused by the diffusion of $Fe(CN)_6^{3-}$ shows strong dependence on ionic strength, nanochannel diameter, charge property of the probe molecule, and DNA concentration. The performance of the present DNA sensor would be further improved if the detection conditions are optimized, including increasing the cDNA length, decreasing the pore diameters of the PAA membrane, or miniaturization of the present system. The present nanochannel array-based DNA senor will lay out prospects for clinical diagnostics and life science research. We believe the present system will have multiple applications in the bioanalytical field.

METHODS

Surface Modification. Porous anodic alumina (PAA) membrane from Whatman with 20 nm pore diameter and 60 μm thickness was first cleaned as described elsewhere.[36] The cleaned PAA was then immersed into a 10 mL acetone solution containing 2.5% 3-aminopropyltriethoxysilane (APTES) for about 1 h with grafting aminopropyl functional groups. After that, excess silane solution was removed from the PAA nanochannels by rinsing with copious amounts of acetone, followed by deionized water wash. The sample was then dried under a stream of nitrogen to remove any impurities and fluid. The remaining modifications (originating on the surface-bound amines) were performed after sputtering an Au film at the 200 nm side of the commercial PAA membranes and the membranes were assembled in the detection cell.

Fabrication of Au Film Working Electrode on PAA Membrane. An Au film working electrode on PAA membrane was fabricated as follows. A 100 nm thick Au film was sputtered on the 200 nm side of the commercial PAA membrane. The Au film sputtering was performed using a current of 15 mA in a vacuum chamber with a pressure of 5×10^{-4} mbar (Ar plasma) for 700 s. To dispose the Au film electrode with ease, the Au film-coated PAA membrane was sandwiched between two poly(ethyleneterephthalate) (PET) sheets (100 μm thick, DIKA Official Limited Company, Suzhou, China) with prepunched 2 mm holes. The holes defined the area of the membrane exposing to the solution phases. Then, a 0.2 mm diameter of Cu wire was placed in electrical contact with the Au film coated PAA membrane by Ag conductive epoxy. Extra care has to be taken so that the Ag conductive epoxy must not touch the exposing area in case it blocks the nanochannels. Finally, the membrane assembly was laminated together by a heating laminator (Zhejiang Huada Limited Company, Zhejiang, China) at 150 °C with the two prepunched holes well aligned.

Cell Assembly and Electrochemical Measurements. The APTES-grafted PAA membrane with an Au film electrode was further functionalized by overnight treatment with 2.5% glutaraldehyde, followed by copious amounts of rinsing and subsequent drying. After the above treatments, glutaraldehyde was successfully covalently coupled onto the surface amine functional groups on PAA, which was further used to covalently bind amine groups of nucleic acid.[2] Then, the membrane was left in a buffer solution for at least 30 min to ensure complete wetting. Then, the fabricated PAA membrane was clamped between two thin poly(dimethylsiloxane) (PDMS) films and then placed between two 2 mL homemade half cells for transport experiments. The two holes of both half cells were aligned to the exposed holes of the PAA membrane (effective transport area, 3.14 mm^2). Importantly, the Au film coated side of the PAA membrane was connected with the permeate cell. The Au film working electrode on the PAA membrane and a Pt wire counter electrode and the Ag/AgCl reference electrode in the permeate cell form a three-electrode electrochemical system for electrochemical detection.

After the two cells (feeding and permeating cells) were filled with 2 mL of 0.5 mM Tris-HCl (pH 8.0) solution, a constant magnetic stirring was applied to the feeding cell. Meanwhile, a potential of 0 V for electrochemical detection of $Fe(CN)_6^{3-}$ was applied to the Au film working electrode using a CHI 900 electrochemical workstation to monitor the current response of the transported $Fe(CN)_6^{3-}$ ions. As soon as 0.03 mM of $Fe(CN)_6^{3-}$ was added in the feeding cell, a significant current increase can be observed because of $Fe(CN)_6^{3-}$ flowing through the nanochannel to the Au film electrode surface. From the signal change after hybridization the target DNA concentration can be recognized.

Immobilization of Nucleic Acid. After the membrane was assembled into the cell, 2 mL of solution was filled into the permeating cell and sealed from leakage. Then, a 20 μL solution of aminated morpholino (5′NH_2-GCT TAG GAT CAT CGA GGT CCA ACC A, ordered from Gene Tools LLC), at a concentration of 100 μM prepared in 20 mM PBS (pH 8.0) was dripped on the exposed 20 nm side of PAA surface in the feeding cell for overnight. This technique prevents a small quantity of morpholino solution from evaporation. After the reaction of aminated morpholino with PAA surface (Supporting Information, Figure S1), the remaining aldehyde group was blocked with 0.2% propylamine solution. After that, the membrane was washed with 0.1 M NaCl and subsequently with deionized water.

Hybridization and Regeneration of DNA Chip. The DNA hybridization was carried out with 30 μL cDNA (5′ TGG TTG GAC CTC GAT GAT CCT AAG, order from shanghai shenggong in China) at various concentrations in 5 × SSC (salt-sodium citrate) buffer solution incubated at morpholino-functionalized membrane for 1 h at room temperature. Later on, the membrane was washed with copious amounts of 0.1 M NaCl to remove unhybridized DNA before performing the electrochemical measurements. The regeneration of the DNA detection device can be achieved by treatment with 9 M urea, followed by buffer solution rinsing.

Characterization. The morphology of PAA was characterized by scanning electron microscopy (SEM, Hitachi, S-4800, 15 kV). X-ray photoelectron spectroscopy (XPS) was used to characterize the immobilization of morpholino in the porous alumina membrane.

Acknowledgment. This work was supported by the grants from the National 973 Basic Research Program (2007CB714501, 2007CB936404), the National Natural Science Foundation of China (NSFC, No. 20828006, 20890020, 21035002, 21005038), the National Science Fund for Creative Research Groups (20821063) and the Ministry of Education of China (200802840012).

Supporting Information Available: The setup used for membrane transport experiment, XPS characterization of morpholino in the PAA membrane, and the influence of ionic strength on the current response of probe molecule transporting through the bare PAA membrane. This material is available free of charge *via* the Internet at http://pubs.acs.org.

REFERENCES AND NOTES

1. Xia, F.; Guo, W.; Mao, Y. D.; Hou, X.; Xue, J.; Xia, H.; Wang, L.; Song, Y.; Ji, H.; Jiang, L.; *et al*. Gating of Single Synthetic Nanopores by Proton-Driven DNA Molecular Motors. *J. Am. Chem. Soc.* **2008**, *130*, 8345–8350.
2. Yameen, B.; Ali, M.; Neumann, R.; Ensinger, W.; Knoll, W.; Azzaroni, O. Synthetic Proton-Gated Ion Channels *via* Single Solid-State Nanochannels Modified with Responsive Polymer Brushes. *Nano Lett.* **2009**, *9*, 2788–2793.
3. Vlassiouk, I.; Kozel, T. R.; Siwy, Z. S. Biosensing with Nanofluidic Diodes. *J. Am. Chem. Soc.* **2009**, *131*, 8211–8220.
4. Umehara, S.; Karhanek, M.; Davis, R. W.; Pourmand, N. Label-free Biosensing with Functionalized Nanopipette Probes. *Proc. Natl. Acad. Sci.* **2009**, *106*, 4611–4616.
5. Karhanek, M.; Kemp, J. T.; Pourmand, N.; Davis, R. W.; Webb, C. D. Single DNA Molecule Detection Using Nanopipettes and Nanoparticles. *Nano Lett.* **2005**, *5*, 403–407.
6. Chen, W.; Wu, J. S.; Xia, X. H. Porous Anodic Alumina with Continuously Manipulated Pore/Cell Size. *ACS Nano* **2008**, *2*, 959–965.
7. Kohli, P.; Harrell, C. C.; Cao, Z. H.; Gasparac, R.; Tan, W. H.; Martin, C. R. DNA-Functionalized Nanotube Membranes with Single-Base Mismatch Selectivity. *Science* **2004**, *305*, 984–986.
8. Hulteen, J. C.; Jirage, K. B.; Martin, C. R. Introducing Chemical Transport Selectivity into Gold Nanotubule Membranes. *J. Am. Chem. Soc.* **1998**, *120*, 6603–6604.
9. Wang, X.; Smirnov, S. Label-Free DNA Sensor Based on Surface Charge Modulated Ionic Conductance. *ACS Nano* **2009**, *3*, 1004–1010.
10. Chen, W.; Yuan, J. H.; Xia, X. H. Characterization and Manipulation of the Electro-osmotic Flow in Porous Anodic Alumina Membranes. *Anal. Chem.* **2005**, *77*, 8102–8108.
11. Hou, X.; Jiang, L. Learning from Nature: Building Bio-inspired Smart Nanochannels. *ACS Nano* **2009**, *3*, 3339–3342.
12. Hou, X.; Guo, W.; Xia, F.; Nie, F. Q.; Dong, H.; Tian, Y.; Wen, L.; Wang, L.; Cao, L.; Jiang, L.; *et al*. A Biomimetic Potassium Responsive Nanochannel: G-Quadruplex DNA Conformational Switching in a Synthetic Nanopore. *J. Am. Chem. Soc.* **2009**, *131*, 7800–7805.
13. Hou, X; Dong, H.; Zhu, D. B.; Jiang, L. Fabrication of Stable Single Nanochannels with Controllable Ionic Rectification. *Small* **2010**, *3*, 361–365.
14. Hou, X.; Liu, Y. J.; Dong, H.; Yang, F.; Li, L.; Jiang, L. A pH-Gating Ionic Transport Nanodevice: Asymmetric Chemical Modification of Single Nanochannels. *Adv. Mater.* **2010**, *22*, 2440–2443.
15. Siwy, Z.; Trofin, L.; Kohli, P.; Baker, L. A.; Trautmann, C.; Martin, C. R. Protein Biosensors Based on Biofunctionalized Conical Gold Nanotubes. *J. Am. Chem. Soc.* **2005**, *127*, 5000–5001.
16. Chen, W.; Wu, Z. Q.; Xia, X. H.; Xu, J. J.; Chen, H. Y. Anomalous Diffusion of Electrically Neutral Molecules in Charged Nanochannels. *Angew. Chem., Int. Ed.* **2010**, *49*, 7943–7947.
17. Schoch, R. B.; Cheow, L. F.; Han, J. Y. Electrical Detection of Fast Reaction Kinetics in Nanochannels with an Induced Flow. *Nano Lett.* **2007**, *7*, 3895–3900.
18. Howorka, S.; Siwy, Z. Nanopore Analytics: Sensing of Single Molecules. *Chem. Soc. Rev.* **2009**, *38*, 2360–2384.
19. Lemay, S. G. Nanopore-Based Biosensors: The Interface Between Ionics and Electronics. *ACS Nano* **2009**, *3*, 775–779.
20. Jagerszki, G.; Gyurcsanyi, R. E.; Hofler, L.; Pretsch, E. Hybridization-Modulated Ion Fluxes through Peptide-Nucleic-Acid-Functionalized Gold Nanotubes. A New Approach to Quantitative Label-free DNA Analysis. *Nano Lett.* **2007**, *7*, 1609–1612.
21. Chen, Q. J.; Zhao, H.; Ming, T.; Wang, J. F.; Wu, C. Nanopore Extrusion-Induced Transition from Spherical to Cylindrical Block Copolymer Micelles. *J. Am. Chem. Soc.* **2009**, *131*, 16650–16651.
22. Summerton, J. E. Morpholinos and PNAs Compared. *Lett. Pept. Sci.* **2004**, *10*, 215–236.
23. Atkins, P. de Paula; J. *Physical Chemistry*, 8th ed.; Oxford: New York, 2006, pp 168−168.
24. Wright, M. R. *An Introduction to Aqueous Electrolyte Solutions*, Wiley: New York, 2007; pp 351−353.
25. Bluhm, E. A.; Bauer, E.; Chamberlin, R. M.; Abney, K. D.; Young, J. S.; Jarvinen, G. D. Surface Effects on Cation Transport across Porous Alumina Membranes. *Langmuir* **1999**, *15*, 8668–8672.
26. Blooomfield, V. A.; Crothers, D. M.; Tinoco, I.; Hearst, J. E.; Wemmer, D. E.; Killman, P. A.; Turner, D. H. *Nucleic Acids: Structures, Properties, and Functions*; University Science Books: Sausalito, CA, 1999; pp 93.
27. Kimura-Suda, H.; Petrovykh, D. Y.; Tarlov, M. J.; Whitman, L. J. Base-Dependent Competitive Adsorption of Single-Stranded DNA on Gold. *J. Am. Chem. Soc.* **2003**, *125*, 9014–9015.
28. Lu, C. H.; Yang, H. H.; Zhu, C. L.; Chen, X.; Chen, G. N. A Graphene Platform for Sensing Biomolecules. *Angew. Chem., Int. Ed.* **2009**, *48*, 1–4.
29. Levicky, R.; Herne, T. M.; Tarlov, M. J.; Satija, S. K. Using Self-Assembly To Control the Structure of DNA Monolayers on Gold: A Neutron Reflectivity Study. *J. Am. Chem. Soc.* **1998**, *120*, 9787–9792.
30. Yang, R. H.; Jin, J. Y.; Chen, Y.; Shao, N.; Kang, H. Z.; Xiao, Z. Y.; Tang, Z. W.; Wu, Y. R.; Zhu, Z.; Tan, W. H. Carbon Nanotube-Quenched Fluorescent Oligonucleotides: Probes that Fluoresce upon Hybridization. *J. Am. Chem. Soc.* **2008**, *130*, 8351–8358.
31. Mukhopadhyay, R. What Does Nanofluidics Have to Offer. *Anal. Chem.* **2006**, *78*, 7379–7382.
32. Vlassiouk, I; Smirnov, S; Siwy, Z. Ionic Selectivity of Single Nanochannels. *Nano Lett.* **2008**, *8*, 1978–1985.
33. Martin, C. R.; Nishizawa, M.; Jirage, K.; Kang, M. Investigations of the Transport Properties of Gold Nanotubule Membranes. *J. Phys. Chem. B* **2001**, *105*, 1925–1934.
34. Gyurcsanyi, R. E. Chemically-Modified Nanopores for Sensing. *Trends Anal. Chem.* **2008**, *27*, 627–639.
35. Bluhm, E. A.; Schroeder, N. C.; Bauer, E.; Fife, J. N.; Chamberlin, R. M.; Abney, K. D.; Young, J. S.; Jarvinen, G. D. Surface Effects on Metal Ion Transport across Porous Alumina Membranes. 2. Trivalent Cations: Am, Tb, Eu, and Fe. *Langmuir* **2000**, *16*, 7056–7060.
36. Nagale, M.; Kim, B. Y.; Bruening, M. L. Ultrathin, Hyperbranched Polymer Membranes. *J. Am. Chem. Soc.* **2000**, *122*, 11670–11678.